



High-efficiency nanowire light-emitting diodes for augmented reality and virtual reality displays

Yizhou Qian, SID Student Member¹ | Zhiyong Yang, SID Student Member¹  |
Yu-Hsin Huang² | Kuan-Heng Lin² | Shin-Tson Wu, SID Fellow¹ 

¹College of Optics and Photonics,
University of Central Florida, Orlando,
Florida, USA

²AU Optronics Corp., Hsinchu, Taiwan

Correspondence

Shin-Tson Wu, College of Optics and
Photonics, University of Central Florida,
Orlando, FL 32816, USA.
Email: swu@creol.ucf.edu

Funding information

a.u.Vista, Inc.

Abstract

Through 3D dipole cloud model, RGB (red, green, and blue) nanowire light-emitting diode (LED) structures are geometrically optimized to exhibit a narrower radiation pattern, weaker angular color shift, and higher optical efficiency. In comparison with micro-LEDs whose external quantum efficiency is dependent on the mesa size, these RGB nanowire LEDs are more efficient than micro-LEDs when the chip size is below 20, 80, and 10 μm , respectively. As a result, nanowire LED is a promising candidate for augmented reality and virtual reality displays where high-resolution density and efficient directional light emission are desired.

KEYWORDS

AR/VR displays, light engines, nanowire LEDs

1 | INTRODUCTION

Nanowire light-emitting diode (LED) is potentially a strong candidate for augmented reality (AR) and virtual reality (VR) light engine.¹ Compared with micro-LEDs whose efficiency degrades as the pixel size decreases,^{2–4} nanowire LEDs can relieve the tradeoff between small pixel size and high external quantum efficiency (EQE).^{5–7} At SID 2018, Aledia reported that the EQE of nanowire LEDs remains a constant when the pitch size is reduced from 1 mm to 5 μm .⁵ Among different nanowire structures, InGaN/GaN dot-in-wire hexagonal LED is attractive due to the support of full-color monolithic integration, reduced dislocation density, and excellent electrical performance.^{8,9} Moreover, its emission wavelength depends on the wire diameter, which in turn can be controlled by the indium concentration.¹⁰ Thus, a full-color display can be achieved by solely changing the nanowire's diameter.

For AR/VR applications, the light emitted from the display panel is collected by a lens before entering the human eye pupil and the accepting cone is typically about

$\pm 20^\circ$.^{11,12} Fortunately, the out-of-plane nanowire structure functions as a waveguide to offer directional light emission. However, due to different emission wavelengths and wire diameters of red, green, and blue (RGB) LEDs, different waveguide modes are excited in the nanowires and each mode has its own outcoupling efficiency.¹³ Thus, the mismatched radiation patterns could cause a severe angular color shift.¹⁴ Therefore, the geometry of each nanowire should be optimized separately to efficiently couple the emitted full-color light to the imaging system. According to our simulation results, RGB nanowires can achieve directional light emission, negligible angular color shift, and high EQE by proper geometrical engineering.

2 | DIPOLE CLOUD SIMULATION VALIDATION

Finite-difference time-domain (FDTD, Ansys Inc.) is employed to perform 3D nanowire simulation with sub-wavelength diameters. Compared with the traditional method that uses a single dipole in the center of the

active layer(s), dipole cloud simulation provides a more accurate result due to the following two reasons: (1) The central dipole method ignores the dipoles close to the edge of the active layer(s), which causes a significant mismatch due to the neglect of high-order mode excited by symmetry breaking; (2) the dipoles close to the edge of the active layer(s) typically have a heavier geometrical weightage. Both methods are applied to a near-infrared cylindrical InP nanowire LED¹⁵ to illustrate their difference. As shown in Figure 1A, the 3D FDTD simulation regime is defined by a steep-angle perfect-matched layer (SA-PML). The nanowire diameter is 230 nm with 2- μm height that includes a 1.2- μm p-InP layer. The active layer is composed of a single layer dipole cloud corresponding to the single quantum well layer. The thickness of resin and top ITO (indium tin oxide) layer is 1.7 μm and 200 nm, respectively. The top of the nanowire is covered with a thin spherical capping of ITO. The dispersion of both InP and ITO is taken into consideration.^{16,17} A 2D power monitor is placed at the top of the nanowire to capture the far-field response. As illustrated by the cross-section view of the active layer in Figure 1B, the dipole cloud is formed by three sets of electric dipoles which are separated by 50 nm along the x-axis from center to edge and each set is composed of x-, y-, and z- polarized dipoles. Note that the optical response of each dipole is calculated separately to avoid perfect coherence in FDTD. Figure 1C compares the normalized polar plot of spectrally integrated electroluminescence (EL) between our simulation results and the experimental data.¹⁵ The emission wavelength is 805–840 nm, which is dominated by

the wurtzite portion of InP nanowire. Therefore, the dipole oscillating along the c-axis (z-axis) is weaker than the other two. The measured peak intensity locates at $\sim 12^\circ$, which is very close to the dipole cloud simulation results. However, the radiation pattern calculated from the center dipole model fails to provide a correct result.

3 | FULL-COLOR InGaN/GaN NANOWIRE

3.1 | Modeling and color performance of full-color InGaN/GaN nanowire

We construct a full-color single InGaN/GaN dot-in-nanowire LED model based on Ra's results.⁸ As indicated in Figure 2A, each nanowire consists of a 300-nm n-GaN layer, 60-nm six vertically aligned InGaN/GaN quantum dots layer, 150-nm p-GaN layer, and 150-nm GaN capping layer with diameter of [blue, green, and red] nanowire to be [630 nm, 420 nm, and 220 nm], respectively. The substrate is covered by the 10-nm hexagonal Ti hole array mask. The dispersion of Ti, GaN, and GaN/InGaN active region are all considered.¹⁸ The nanowire except the capping is immersed in polyimide whose refractive index is 1.5. Table 1 lists the material properties at the center wavelength of each primary color in the simulation.

Like Section 2, the FDTD simulation region is defined by SA-PML. A large 3D emission box monitor is placed around the structure in air to calculate the emission

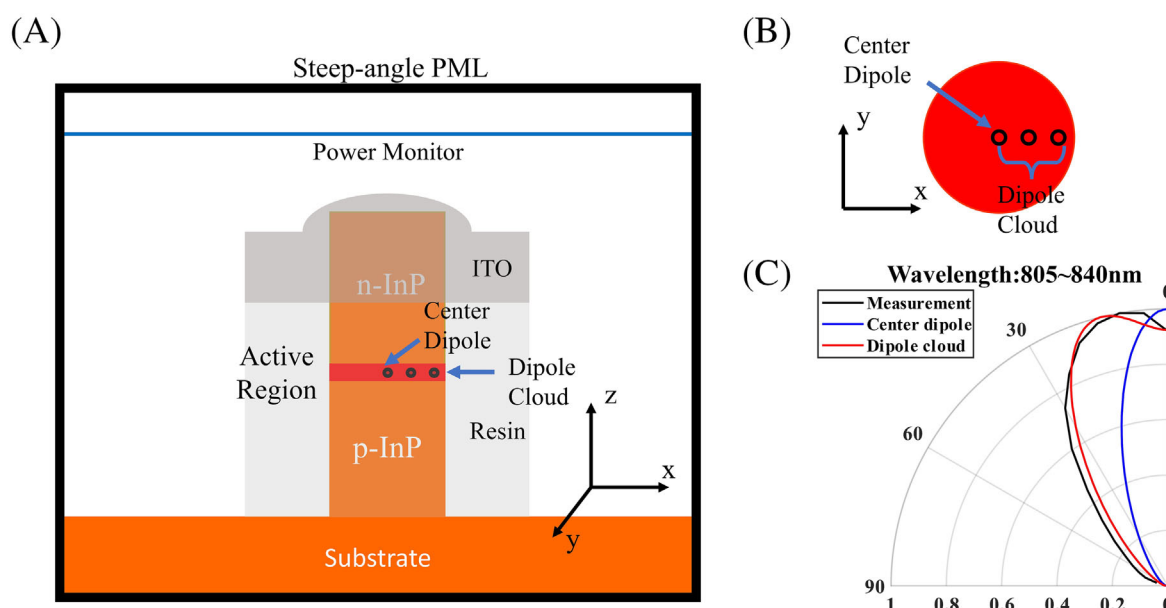


FIGURE 1 (A) 3D-FDTD InP nanowire LED simulation schematic, (B) cross-sectional view of active layer, and (C) simulated far-field radiation patterns of InP nanowire LED. The experimental data (black curve) included for comparison is from Motohisa et al.¹⁵

FIGURE 2 (A) Schematic of FDTD simulation model in X-Z plane. (B) Top view of blue, green, and red active layer in hexagonal nanowire LED with a different diameter.

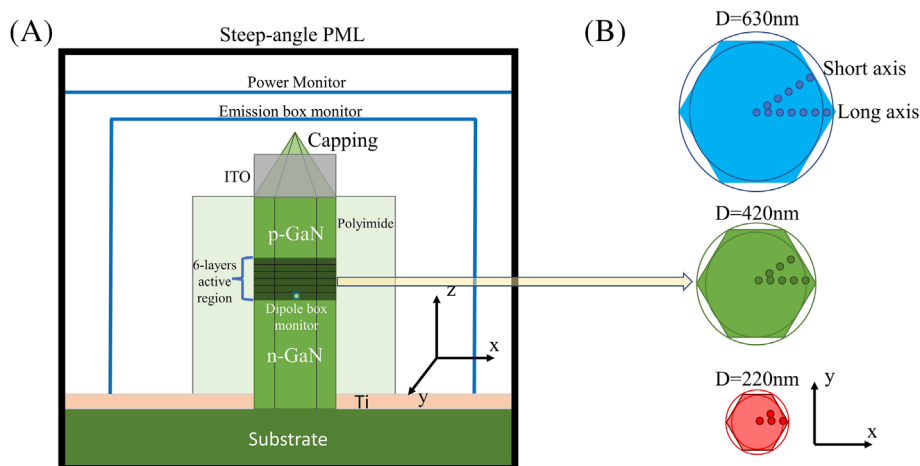


TABLE 1 FDTD material parameters in Section 3.1 for InGaN/GaN nanowire LED.

Material	Blue (460 nm)		Green (530 nm)		Red (660 nm)	
	n	k	n	k	n	k
GaN	2.49	-	2.40	-	2.37	-
MQW	2.54	-	2.41	-	2.35	-
Ti	1.68	2.25	1.84	2.52	2.25	3.02

power of the nanowire. The substrate side of the large 3D box monitor is open to get rid of the substrate loss. Small 3D box monitors are placed surrounding each dipole source to receive the dipole power. Therefore, the light extraction efficiency (LEE) can be found from the ratio of power calculated from the emission box monitor to the dipole monitor.

In x-y plane, due to the hexagonal structure, dipoles are divided into two directions: short axis and long axis, which are defined by the inscribed circle and circumscribed circle, respectively, and we denote this axis dependence to be L and S. As shown in Figure 2B, each adjacent dipole in a blue nanowire LED is separated by 50 nm along the axis; thus, the short axis and long axis consist of six and seven dipoles, respectively. Similarly, for green nanowire LEDs, four dipoles are simulated along short axis, and five dipoles are considered for long axis. For red LEDs, the total response consists of two dipoles for short axis and three dipoles for long axis. Since the GaN crystal structure is wurtzite and the dipoles oscillating along c-axis is neglected,¹⁹ therefore, two polarizations of dipoles are considered: in-axis and out-of-axis, denoted as I and O, respectively.

The emission wavelength of dipole sources follows the unfiltered emission spectra (solid lines in Figure 3A) measured and reported in Ra et al.⁸ to

calculate LEE. However, in the far-field, the color performance of InGaN/GaN-based nanowire LED is limited. All the three nanowires without color filters have strong side lobe emissions because the indium adatom diffusion is difficult to be controlled perfectly. In addition, the red nanowire emission spectrum is relatively broad (FWHM ~ 120 nm) since it is formed by InGaN. After applying color filters above the nanowires (dashed lines in Figure 3A), the suppression of side lobe emission significantly increases the color purity and enlarges the color gamut as Figure 3B shows. Without color filters, the nanowire LED only covers 55.7% DCI-P3 color space and 40.6% Rec.2020, while it can cover 118.5% DCI-P3 and 86.4% Rec.2020 after applying color filters.

3.2 | Angular distribution and LEE calculations

In 3D FDTD simulation, the angular distribution collected from 2D power monitor is azimuthal angle φ , polar angle θ , wavelength λ , polarization p (in-axis I or out-of-axis O), simulation axis a (long-axis L or short-axis S), and position dependent (x, z). However, the final emission result should only be a function of (θ , φ). Here, we first eliminate wavelength and

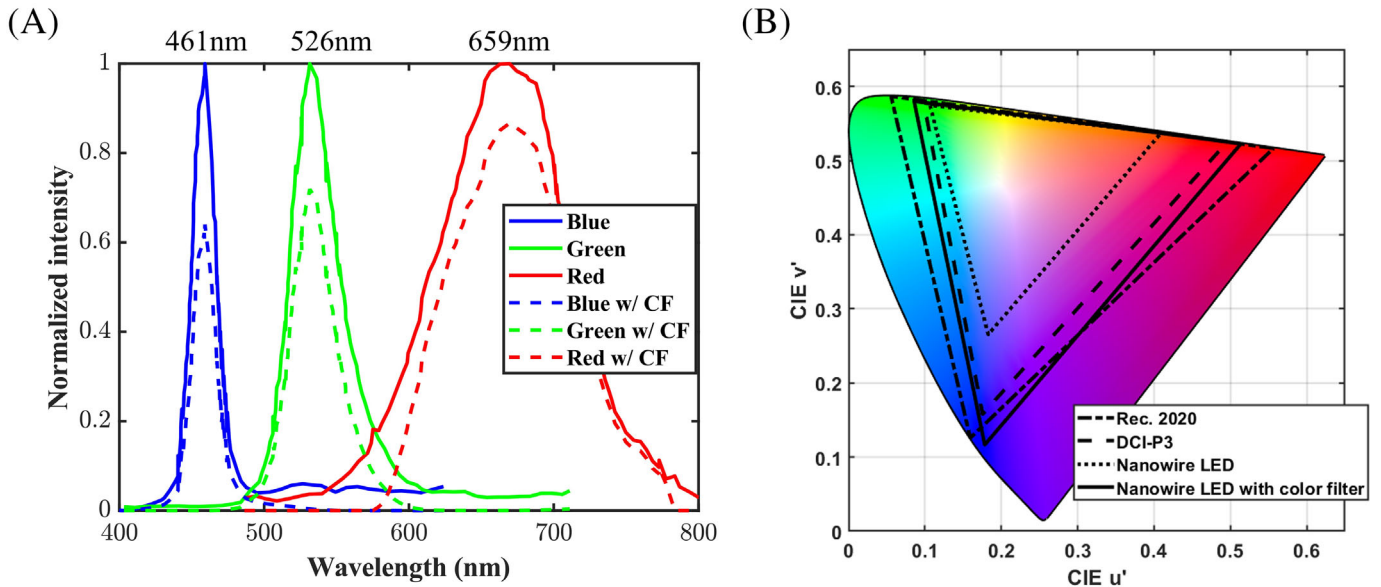


FIGURE 3 (A) Measured EL spectra of single nanowire LEDs with different diameters from Ra et al.⁸ (B) Simulated color triangle of the GaN/InGaN nanowire LED display.

polarization dependence by (1) multiplying the weightage of each wavelength and (2) averaging each dipole polarization.^{20,21}

$$A1(\theta, \varphi, x, z, a) = \frac{\sum_{p=I,O} \int A(\theta, \varphi, x, z, \lambda, p, a) S(\lambda) d\lambda}{2 \int S(\lambda) d\lambda}, \quad (1)$$

where $S(\lambda)$ is the emission spectrum without color filter as shown in Figure 3A. The position-averaged angular distribution for long axis (A_{2L}) and short axis (A_{2S}) can be calculated as

$$A_{2L}(\theta, \varphi) = \frac{\sum_{z=1}^6 \int_0^{R_L} A_{1L}(\theta, \varphi, x, z) 2\pi x dx}{6\pi R_L^2}, \quad (2a)$$

$$A_{2S}(\theta, \varphi) = \frac{\sum_{z=1}^6 \int_0^{R_S} A_{1S}(\theta, \varphi, x, z) 2\pi x dx}{6\pi R_L^2}, \quad (2b)$$

where R_L and R_S are radius of the circumscribed circle and inscribed circle, respectively. The total angular distribution can be obtained from the summation of all the short and long axes dipole responses.

In AR waveguide, a large optical power collimation lens is required to achieve a large field-of-view for

microdisplays. However, the small f -number lens is limited by its physical size, resulting in an accepting cone of about $\pm 20^\circ$. Therefore, we define the effective LEE to be the LEE received within $\pm 20^\circ$ in the far-field; otherwise, the light would not be received by the imaging system. Therefore, the wavelength and polarization independent effective LEE can be expressed as

$$\eta_{(20)}(x, z, a) = \frac{\sum_{p=I,O} \int r_{(20)}(x, z, \lambda, p, a) \frac{P_E(x, z, \lambda, p, a)}{P_D(x, z, \lambda, p, a)} S(\lambda) d\lambda}{2 \int S(\lambda) d\lambda}, \quad (3)$$

where $r_{(20)}$ is the $\pm 20^\circ$ spectral ratio, P_E is the total emission power, and P_D is the total dipole power as mentioned in Section 3.1. The calculation of position-averaged effective LEE for long and short axis dipole responses are similar to Equations (2a) and (2b). The total LEE is the summation of both axis dipole responses.

3.3 | Light emission from unoptimized nanowire LEDs

Based on FDTD simulation results in Section 2 and the equations in Section 3, we calculate the normalized 2D angular distribution for blue, green, and red nanowire LEDs in Figure 4A–C, respectively. Among these nanowire LEDs, the blue nanowire (Figure 4A) shows

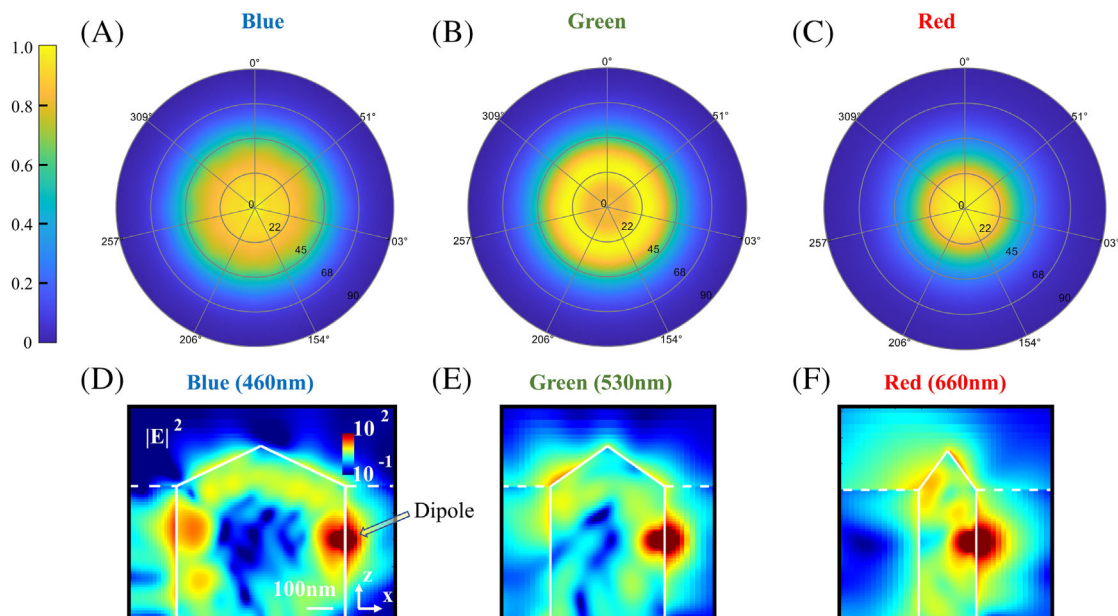


FIGURE 4 (A–C) Normalized 2D angular distribution for (A) blue, (B) green, and (C) red LEDs. (D–F) Calculated distribution maps of $|E|^2$ at the capping layer with x-polarized edge dipoles for (D) blue, (E) green, and (F) red nanowire LEDs.

the broadest angular distribution because high-order waveguide modes can be easily excited in waveguides with a large diameter. Besides, the light intensity in the center of the green nanowire is weaker than its counterpart at $\sim 20^\circ$ to 40° (Figure 4B), which is also known as batwing profile. On the other hand, the red nanowire LED (Figure 4C) shows the narrowest spectrum. According to Equation (3), the effective LEE of [blue, green, and red] nanowire LEDs is [9.3%, 18.8%, and 30.6%], respectively. Similarly, the substrate loss is calculated as [29.0%, 41.9%, and 31.6%].

To better understand the light emission from the hexagonal waveguide, we plot the electric field intensity of the selected x-polarized long-axis dipoles in Figure 4D–F for blue, green, and red nanowires, respectively. Note that the edge dipoles are picked because they have the heaviest geometrical weightage as Equation (2a) implies. Figure 4D indicates that a large portion of light escapes from the waveguide through the sidewall instead of emitting from top of the blue nanowire. Therefore, a broad angular distribution and a large loss can be expected. For green nanowire LEDs (Figure 4E), light is mostly emitted from the capping with a tilted angle, which results in a batwing profile. Compared with the other two cases, red nanowire (Figure 4F) is more efficient in concentrating light in normal direction and the leakage loss from the sidewall is suppressed. Additionally, the mismatched angular distribution between RGB nanowire LEDs will introduce angular color shift, which will be discussed in Section 3.5.

3.4 | Optimization

It should be mentioned that there are several constraints during the optimization process. First, the nanowire diameter must be fixed; otherwise, the emission wavelength will be different due to the change of indium adatom diffusion. Second, the height of the RGB nanowire main body should be identical because the electrodes are fabricated at the same height in real applications. Therefore, we design our optimization process in two aspects: (1) changing the n-GaN and p-GaN layer thickness simultaneously and (2) modifying the capping layer height. The n-GaN/p-GaN layer thickness controls the interference between the dipoles in active layer and their reflection from the GaN-Ti and GaN-air interfaces. Additionally, p-GaN capping thickness determines the outcoupling efficiency of light from the waveguide into air. Therefore, we designed a two-dimensional sweeping of (1) the vertical position of the active layer by changing the bottom n-GaN thickness with 10-nm step and (2) the p-GaN capping height from 0 to 150 nm with 30-nm step. Here, we only focus on the optimization of edge dipoles on long axis due to our limited computer memory.

As indicated in the top figures of Figure 5A–C, increasing capping height consistently broadens the angular distribution for all the cases because the emitted light from the nanowire waveguide is tilted by the capping; therefore, we remove the capping layer in our design. On the other hand, a narrower angular distribution does not necessarily equal to a higher effective LEE;

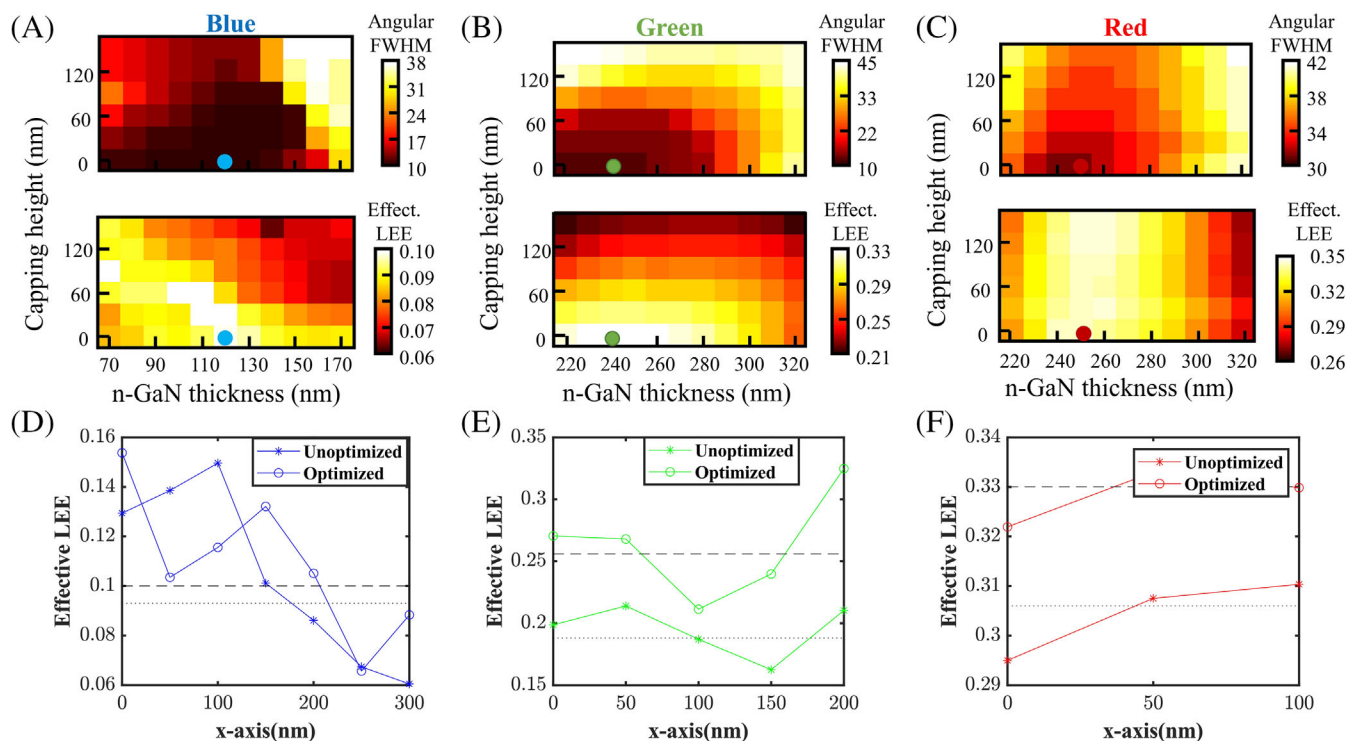


FIGURE 5 (A–C) 2D colormap of top: angular FWHM and bottom: effective LEE as a function of n-GaN thickness and p-GaN capping height: (A) blue, (B) green, and (C) red nanowire LEDs. (D–F) Dependence of effective LEE on the dipole source position along x-axis for (D) blue, (E) green, and (F) red nanowire LEDs. Horizontal lines: radius-averaged effective LEE before optimization (dotted) and after optimization (dashed).

thus, we plot the 2D colormaps of effective LEE based on Equation (3). Results are shown in the bottom figures of Figure 5A–C. Based on these results, we find that the optimized values for [blue, green, and red] nanowire LEDs are (1) to remove the p-GaN capping completely for all the cases and (2) to set n-GaN thickness at [120, 240, 250] nm, respectively.

Based on the optimized geometrical values, 3D dipole cloud is simulated for each case. As calculated from Equation (3), the effective LEE of [blue, green, and red] nanowire LEDs increases from [9.3%, 18.8%, and 30.6%] to [10.0%, 25.6%, and 33.0%], respectively. As shown in Figure 5D–F, due to the competition between radial mode and whispering gallery mode, the effective LEE significantly fluctuates with the variation of the dipole's position along x-axis and the results agree well with previous simulation works.²⁰ For blue nanowire LEDs as Figure 5D depicts, the increment of effective LEE is mainly dominated by the edge dipole. The excitation of high order modes makes it difficult to achieve the highest effective LEE for all the dipoles simultaneously. On the other hand, the effective LEE of green nanowire LEDs (Figure 5E) can be improved significantly if the batwing profile is eliminated. For red nanowire LEDs, although the geometry of the unoptimized nanowire is already

showing a reasonably good performance, the efficiency of all the dipoles can still improve by $\sim 10\%$, as indicated in Figure 5F. The loss on the substrate side is calculated as [30.2%, 42.0%, and 32.5%] for [blue, green, and red] nanowires, which is close to unoptimized nanowires.

3.5 | Performance

Since the 2D angular distribution is almost circularly symmetric after considering both long-axis and short-axis dipoles, 1D angular distribution ($\varphi = 0^\circ$) can provide a fair comparison between unoptimized and optimized cases. As depicted in Figure 6A, in contrast to unoptimized data (solid lines), the optimized angular distribution (dashed lines) shows a better angular match within the accepting cone ($\theta = 0^\circ\text{--}20^\circ$). Remarkably, the batwing profile of the green nanowire is eliminated and the angular FWHM of [blue, green, and red] nanowires is reduced from [48°, 47°, and 35°] to [37°, 33°, and 24°], respectively. Figure 6B,C describes the $\pm 20^\circ$ angular color shift of 18 reference colors in Macbeth Color-Checker for unoptimized and optimized nanowire LEDs,²² respectively. After optimization, the angular color shift, especially for green mixed colors, is

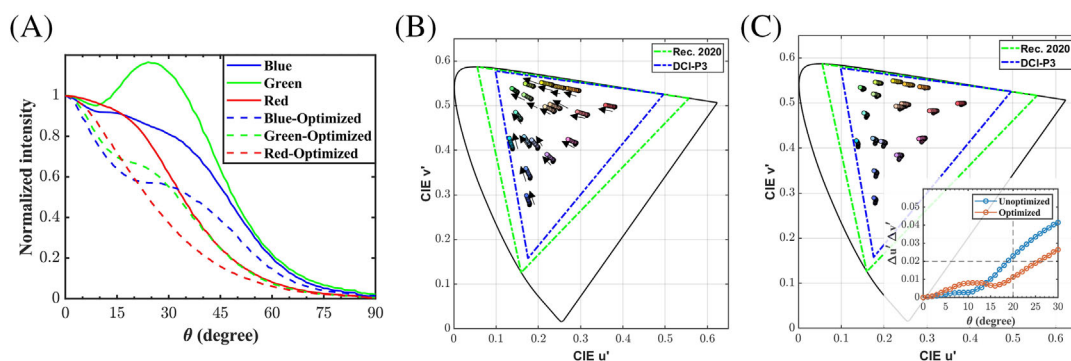
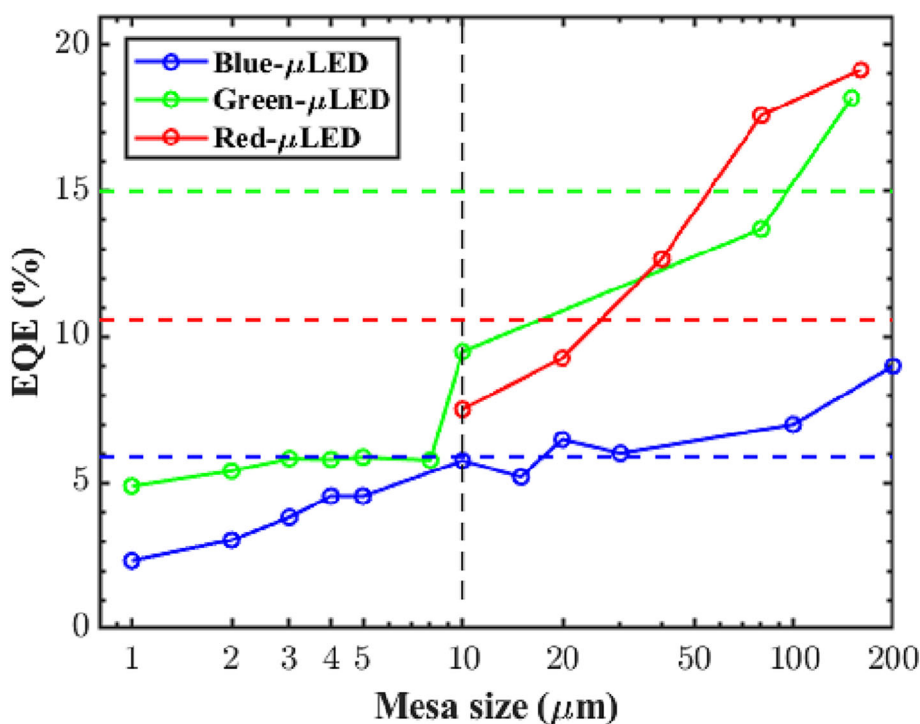


FIGURE 6 (A) Comparison of normalized 1D angular distribution between unoptimized (solid lines) and optimized (dash lines) nanowire LEDs. (B, C) Simulated angular color shift of 18 reference colors from 0° to 20° (B) before and (C) after optimization. (Inset) Simulated average color shift from 0° to 30° viewing angle after optimization.

FIGURE 7 Comparison between calculated effective EQE of nanowire LED (horizontal dashed lines) with measured EQE of blue InGaN μ LEDs from Smith et al.²⁵ and Olivier et al.,²⁶ green InGaN μ LEDs from previous studies,^{25,27–29} and red AlGaInP μ LEDs from Fan et al.³⁰ as a function of mesa diameter. Vertical dashed lines: EQE of μ LEDs with 10- μ m mesa size.



suppressed due to the elimination of batwing profile. The inset in Figure 6C shows that the average $\pm 20^\circ$ color shift of unoptimized nanowires is $\Delta u' \Delta v' = 0.023$, which exceeds human just-noticeable level ($\Delta u' \Delta v' = 0.02$), while the $\pm 20^\circ$ color shift is only 0.013 for the optimized nanowires. Remarkably, the color shift is not observable until $\theta > 25^\circ$, which is already beyond the current accepting cone for AR applications.

As mentioned in Section 3.4, the effective LEE of [blue, green, and red] nanowire LEDs increases from [9.3%, 18.8%, and 30.6%] to [10.0%, 25.6%, and 33.0%], respectively. If the blue and green InGaN/GaN nanowire LEDs can achieve 58.5% IQE²³ and red nanowire LED can achieve 32.2% IQE,²⁴ then the corresponding effective EQE for AR applications will be [blue, green,

and red] = [5.9%, 15.0%, and 10.6%]. For μ LEDs, its EQE decreases as the mesa size decreases due to side-wall defects and surface recombination. Even if we assume that all the produced light from μ LEDs can be coupled into the AR/VR imaging system, in comparison with blue^{25,26} and green InGaN μ LEDs^{25,27–29} in which EQE is size dependent, our blue nanowire LED still has a higher EQE than μ LED whose mesa size is smaller than 10 μ m as shown in Figure 7. The advantage of nanowire is pronounced for green light emission and the effective LEE of green nanowire LEDs is even higher than that of 80- μ m μ LED. For red light emission, InGaN/GaN can only achieve 32.2% IQE; however, compared with AlGaInP red μ LEDs,³⁰ our red nanowire LED shows a higher EQE than that with

20- μm mesa size because of its exceedingly high effective LEE. For a display panel consisting of RGB μLEDs with 10- μm mesa size, our [blue, green, and red] nanowire LED offers [1 \times , 1.6 \times , and 1.4 \times] higher efficiency, respectively. In other words, considering sub-pixel rendering, when the resolution density of the full-color display panel exceeds 1270 PPI, nanowire LEDs can always provide a higher efficiency than μLEDs . As the resolution density further increases, the advantage of nanowire LEDs is more pronounced than μLED , which makes nanowire LED an efficient directional light engine for AR/VR displays.

4 | CONCLUSION

In this work, we have simulated, calculated, and optimized the angular distribution and effective LEE of full-color InGaN/GaN nanowire LEDs by 3D dipole cloud simulation. In such a display system, color filters are applied to enlarge the color gamut. By removing the capping and modifying the position of the active layers, the angular color shift within $\pm 20^\circ$ is eliminated and the effective LEE of [blue, green, and red] nanowire LEDs increases from [9.3%, 18.8%, and 30.6%] to [10.0%, 25.6%, and 33.0%], respectively. Compared with RGB μLEDs for AR/VR applications, nanowire LEDs can achieve a higher efficiency when the resolution density of the full-color display panel exceeds 1270 PPI.

ACKNOWLEDGMENT

The UCF group is indebted to a.u.Vista, Inc. for the financial support.

ORCID

Zhiyong Yang  <https://orcid.org/0000-0002-7181-7443>

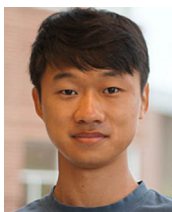
Shin-Tson Wu  <https://orcid.org/0000-0002-0943-0440>

REFERENCES

- Xiong J, Hsiang E-L, He Z, Zhan T, Wu S-T. Augmented reality and virtual reality displays: emerging technologies and future perspectives. *Light Sci Appl*. 2021;10(1):216. <https://doi.org/10.1038/s41377-021-00658-8>
- Huang Y, Hsiang E-L, Deng M-Y, Wu S-T. Mini-LED, micro-LED and OLED displays: present status and future perspectives. *Light Sci Appl*. 2020;9(1):105. <https://doi.org/10.1038/s41377-020-0341-9>
- Olivier F, Daami A, Licitra C, Templier F. Shockley-read-hall and auger non-radiative recombination in GaN based LEDs: a size effect study. *Appl Phys Lett*. 2017;111(2):022104. <https://doi.org/10.1063/1.4993741>
- Boussadi Y, Rochat N, Barnes J-P, Bakir BB, Ferrandis P, Masenelli B, et al. Investigation of sidewall damage induced by reactive ion etching on AlGaInP MESA for micro-LED application. *JOL*. 2021;234:117937. <https://doi.org/10.1016/j.jlumin.2021.117937>
- Gilet P, Robin I-C. 52-1: invited paper: nanostructures on silicon to solve the active display paradigms. *SID Int Symp Dig Tech Pap*. 2018;49(1):684–687. <https://doi.org/10.1002/sdtp.12349>
- Zhao S, Nguyen HP, Kibria MG, Mi Z. III-nitride nanowire optoelectronics. *Prog Quant Electron*. 2015;44:14–68. <https://doi.org/10.1016/j.pquantelec.2015.11.001>
- Zhou X, Tian P, Sher C-W, Wu J, Liu H, Liu R, et al. Growth, transfer printing and colour conversion techniques towards full-colour micro-LED display. *Prog Quant Electron*. 2020;71:100263. <https://doi.org/10.1016/j.pquantelec.2020.100263>
- Ra Y-H, Wang R, Woo SY, Djavid M, Sadaf SM, Lee J, et al. Full-color single nanowire pixels for projection displays. *Nano Lett*. 2016;16(7):4608–4615. <https://doi.org/10.1021/acs.nanolett.6b01929>
- Liu X, Sun Y, Malhotra Y, Wu Y, Mi Z. Monolithic integration of multicolor InGaN LEDs with uniform luminescence emission. *Opt Express*. 2021;29(21):32826–32832. <https://doi.org/10.1364/OE.435871>
- Sekiguchi H, Kishino K, Kikuchi A. Emission color control from blue to red with nanocolumn diameter of InGaN/GaN nanocolumn arrays grown on same substrate. *Appl Phys Lett*. 2010;96(23):231104. <https://doi.org/10.1063/1.3443734>
- Zhan T, Hsiang E-L, Li K, Wu S-T. Enhancing the optical efficiency of near-eye displays with liquid crystal optics. *Crystals*. 2021;11(2):107. <https://doi.org/10.3390/cryst11020107>
- Zou J, Zhan T, Hsiang E-L, Du X, Yu X, Li K, et al. Doubling the optical efficiency of VR systems with a directional backlight and a diffractive deflection film. *Opt Express*. 2021;29(13):20673–20686. <https://doi.org/10.1364/OE.430920>
- Mangalgi GM, Manley P, Riedel W, Schmid M. Dielectric nanorod scattering and its influence on material interfaces. *Sci Rep-UK*. 2017;7(1):4311. <https://doi.org/10.1038/s41598-017-03721-w>
- Gou F, Hsiang E-L, Tan G, Chou P-T, Li Y-L, Lan Y-F, et al. Angular color shift of micro-LED displays. *Opt Express*. 2019;27(12):A746–57. <https://doi.org/10.1364/OE.27.00A746>
- Motohisa J, Kohashi Y, Maeda S. Far-field emission patterns of nanowire light-emitting diodes. *Nano Lett*. 2014;14(6):3653–3660. <https://doi.org/10.1021/nl501438r>
- Dinges H, Burkhard H, Lösch R, Nickel H, Schlapp W. Refractive indices of InAlAs and InGaAs/InP from 250 to 1900 nm determined by spectroscopic ellipsometry. *Appl Surf Sci*. 1992;54:477–481. [https://doi.org/10.1016/0169-4332\(92\)90090-K](https://doi.org/10.1016/0169-4332(92)90090-K)
- Konig TA, Ledin PA, Kerszulis J, Mahmoud MA, El-Sayed MA, Reynolds JR, et al. Electrically tunable plasmonic behavior of nanocube-polymer nanomaterials induced by a redox-active electrochromic polymer. *ACS Nano*. 2014;8(6):6182–6192. <https://doi.org/10.1021/nn501601e>
- Liu Z, Wang K, Luo X, Liu S. Precise optical modeling of blue light-emitting diodes by Monte Carlo ray-tracing. *Opt Express*. 2010;18(9):9398–9412. <https://doi.org/10.1364/OE.18.009398>
- Krames MR, Shchekin OB, Mueller-Mach R, Mueller GO, Zhou L, Harbers G, et al. Status and future of high-power light-emitting diodes for solid-state lighting. *J Disp Technol*. 2007;3(2):160–175. <https://doi.org/10.1109/JDT.2007.895339>

20. Ryu H-Y. Evaluation of light extraction efficiency of GaN-based nanorod light-emitting diodes by averaging over source positions and polarizations. *Crystals*. 2018;8(1):27. <https://doi.org/10.3390/cryst8010027>
21. Qian Y, Yang Z, Huang Y-H, Lin K-H, Wu S-T. Directional high-efficiency nanowire LEDs with reduced angular color shift for AR and VR displays. *Opto-Electronic Sci*. 2022;1(12):220021. <https://doi.org/10.29026/oes.2022.220021>
22. McCamy CS, Marcus H, Davidson JG. A color-rendition chart. *J App Photog Eng*. 1976;2(3):95–99.
23. Jain B, Velpula RT, Bui HQT, Nguyen H-D, Lenka TR, Nguyen TK, et al. High performance electron blocking layer-free InGa_N/GaN nanowire white-light-emitting diodes. *Opt Express*. 2020;28(1):665–675. <https://doi.org/10.1364/OE.28.000665>
24. Nguyen HPT, Zhang S, Cui K, Korinek A, Botton GA, Mi Z. High-efficiency InGa_N/GaN dot-in-a-wire red light-emitting diodes. *IEEE Photonics Tech L*. 2011;24(4):321–323. <https://doi.org/10.1109/LPT.2011.2178091>
25. Smith JM, Ley R, Wong MS, Baek YH, Kang JH, Kim CH, et al. Comparison of size-dependent characteristics of blue and green InGa_N microLEDs down to 1 μm in diameter. *Appl Phys Lett*. 2020;116(7):071102. <https://doi.org/10.1063/1.5144819>
26. Olivier F, Tirano S, Dupré L, Aventurier B, Largeton C, Templier F. Influence of size-reduction on the performances of GaN-based micro-LEDs for display application. *JOL*. 2017;191:112–116. <https://doi.org/10.1016/j.jlumin.2016.09.052>
27. Templier F. GaN-based emissive microdisplays: a very promising technology for compact, ultra-high brightness display systems. *J Soc Inf Disp*. 2016;24(11):669–675. <https://doi.org/10.1002/jsid.516>
28. Zhanghu M, Hyun B-R, Jiang F, Liu Z. Ultra-bright green InGa_N micro-LEDs with brightness over 10M nits. *Opt Express*. 2022;30(6):10119–10125. <https://doi.org/10.1364/OE.451509>
29. Wang L, Wang L, Chen CJ, Chen KC, Hao Z, Luo Y, et al. Green InGa_N quantum dots breaking through efficiency and bandwidth bottlenecks of micro-LEDs. *Laser Photon Rev*. 2021;15(5):2000406. <https://doi.org/10.1002/lpor.202000406>
30. Fan K, Tao J, Zhao Y, Li P, Sun W, Zhu L, et al. Size effects of AlGaInP red vertical micro-LEDs on silicon substrate. *Results Phys*. 2022;36:105449. <https://doi.org/10.1016/j.rinp.2022.105449>

AUTHOR BIOGRAPHIES



Yizhou Qian received his BS degree from Virginia Tech, Blacksburg, Virginia, USA, in 2018 and MEng degree from Virginia Tech, Blacksburg, Virginia, USA, in 2021. Currently, he is working toward the PhD degree at College of Optics and Photonics, University of Central Florida, Florida, USA. His current research focuses on micro-LED, OLED, and mini-LED backlight for light engines for AR/VR display systems and flat panel displays.



Zhiyong Yang received his BS degree in Optoelectronic Engineering from Chongqing University in 2017 and MS degree in Optics & Photonic from the University of Michigan in 2019. Currently, he is working toward a PhD degree from the College of Optics and Photonics, University of Central Florida. His current research interests include liquid-crystal-on-silicon, mini-LED backlight, OLED display, and micro-LED display.

Yu-Hsin Huang received his BS degree from Department of Photonics, National Sun-Yat Sen University, in 2015, and PhD degree from Graduate Institute of Electronics Engineering, National Taiwan University, in 2020. Currently, he is a senior engineer at AUO Corporation, and his R&D interest is in micro-LED optics and display technologies.

Kuan-Heng Lin received his BS degree from Department of Physics, National Chung-Cheng University, in 2003, and MS degree from Department of Photonics, National Chiao-Tung University, in 2009. Currently, he is a manager at AUO Corporation, and his R&D interest is in micro-LED/OLEDs devices and self-emission display technologies.



Shin-Tson Wu is a Trustee Chair professor at the College of Optics and Photonics, University of Central Florida (UCF). He is an Academician of Academia Sinica, a Charter Fellow of the National Academy of Inventors, and a Fellow of the IEEE, OSA, SID, and SPIE. He is a recipient of the Optica Edwin H. Land Medal (2022), SPIE Maria Goepfert-Mayer Award (2022), Optica Esther Hoffman Beller Medal (2014), SID Slottow-Owaki Prize (2011), Optica Joseph Fraunhofer Award (2010), SPIE G. G. Stokes Award (2008), and SID Jan Rajchman Prize (2008). In the past, he served as the founding Editor-In-Chief of the *Journal of Display Technology*, Optica publications council chair and board member, and SID honors and awards committee chair.

How to cite this article: Qian Y, Yang Z, Huang Y-H, Lin K-H, Wu S-T. High-efficiency nanowire light-emitting diodes for augmented reality and virtual reality displays. *J Soc Inf Display*. 2023;31(5):211–19. <https://doi.org/10.1002/jsid.1211>